Ab initio study of the reaction mechanism of CO_2 with Ti atom in the ground and excited electronic states

Der-Yan Hwang
Department of Chemistry, Tamkang University, Tamsui 25137, Taiwan

Alexander M. Mebel
Institute of Atomic and Molecular Sciences, Academia Sinica, P.O. Box 23-166, Taipei 10764, Taiwan

(Received 1 October 2001; accepted 7 January 2002)

Density functional B3LYP/6-311+G(3*df*)//B3LYP/6-31G* calculations of potential energy surfaces (PES) have been performed for the $Ti+CO_2 \rightarrow TiO+CO$ reaction in the triplet, quintet, and singlet electronic states. The results indicate that in the ground triplet state the most favorable reaction mechanism involves insertion of the Ti atom into a CO bond [via a η^2-C,O coordinated *t*-(TiOC)O complex] to produce a triplet *t*-OTiCO molecule with the energy gain of 43.9 kcal/mol and the latter can further dissociate to $TiO(^3\Delta)+CO$ with the total reaction exothermicity of ~30 kcal/mol. The addition mechanism leading to the same $TiO(^3\Delta)+CO$ products via a metastable η^2-O,O complex *t*-cyc-$TiCO_2$ is also feasible at ambient temperatures since the highest barrier on the reaction pathway is only 4.7 kcal/mol. The reaction mechanisms in excited singlet and quintet electronic states have many similar features with the ground state reaction but also exhibit some differences. In the singlet state, the reaction can follow $^1A''$ and $^1A'$ pathways, of those the insertion via a *s*-(TiOC)O ($^1A'$) complex leading to *s*-OTiCO ($^1A'$) and then to $TiO(^1\Delta)+CO$ does not have an activation barrier. The insertion mechanism on the $^1A''$ PES depicts a low barrier of 1.8 kcal/mol and leads to *s*-OTiCO ($^1A''$), which dissociates into $TiO(^1\Delta)+CO$. The addition pathways via η^2-O,O coordinated complexes require to overcome significant barriers, 7.8 and 34.9 kcal/mol for the $^1A''$ and $^1A'$ states, respectively. In the quintet state, the reaction at low and ambient temperatures can proceed only by coordination of Ti(^5F) toward CO_2 with formation of η^2-C,O *q*-(TiOC)O, η^2-O,O *q*-cyc-$TiCO_2$, and η^1-O *q*-TiOCO bound by 9.7, 6.1, and 4.6 kcal/mol, respectively, relative to the reactants. The η^2-C,O and η^1-O coordinations occur without barriers, while the η^2-O,O coordination has an entrance barrier of 4.2 kcal/mol. The calculated PESs show that the carbon dioxide reforming into CO in the presence of Ti atoms should take place spontaneously. © *2002 American Institute of Physics.* [DOI: 10.1063/1.1453954]

I. INTRODUCTION

Many important chemical reactions are catalyzed by transition metals, either homogeneously or heterogeneously. The mechanisms of catalytic reactions involving transition metals therefore represent a research topic of a great interest. Carbon dioxide is normally a very stable species and its reforming into useful organic compounds requires a large amount of energy. The reforming processes can be however substantially enhanced in the presence of transition metals or their complexes and the coordination of the carbon dioxide to the metal center has been considered as a key step.[1–3] In this view, it is important to understand how various metal atoms can react with CO_2. Therefore, the interaction between metal atoms and CO_2 has become an attractive subject of numerous experimental and theoretical studies.[4–26] For instance, matrix isolation spectroscopic experiments have been performed for the reactions of carbon dioxide with first-row transition metals.[4,19–23] They showed a striking difference between the late transition metal atoms (Fe, Co, Ni, and Cu), which formed M(CO_2) complexes, and early transition metals (Sc, Ti, V, and Cr), which spontaneously inserted into a CO bond yielding OMCO species. The OMCO insertion product can decompose into MO+CO or attach another CO_2 molecule with formation of more complicated complexes. The difference can be in part rationalized based on the heats of the $M+CO_2 \rightarrow MO+CO$ reactions, which are exothermic for Sc, Ti, and V but highly endothermic for the late transition metals.[27] A deeper insight into the reaction mechanism can be obtained by *ab initio* and density functional calculations of the reaction potential energy surfaces (PES).

Recently,[28] we carried out theoretical calculations of PES for the $Ni(3d^84s^2,{}^3F)+CO_2 \rightarrow NiO(^3\Sigma^-)+CO$ reaction and showed that this reaction can proceed by addition of the Ni atom to the carbon dioxide to form a C_{2v}-symmetric four-member ring $NiCO_2$ complex (η^2-O,O), which can rearrange to a linear CONiO molecule and then eventually decompose to NiO+CO. The reaction is endothermic by ~36 kcal/mol, and all intermediate steps appeared to be endothermic as well; the cyclic $NiCO_2$ and linear CONiO molecules lie 17–37 kcal/mol above the reactants at different levels of theory and the barrier for the last reaction step reaches ~50–60 kcal/mol relative to $Ni+CO_2$. Earlier combined matrix isolation and density functional studies by Galan *et al.*[25] showed that a singlet side-on (η^2-C,O) $NiCO_2$ complex is the global minimum on the PES, with the binding energy of ~18 kcal/mol. Interestingly, the $M+CO_2 \rightarrow MO$

+CO reaction mechanisms for various alkaline–earth atoms are rather similar to that for M=Ni. Our earlier calculations[29] demonstrated that these reactions proceed by formation of the cyclic MCO_2 intermediate with the η^2-O,O orientation (exothermic for M=Be, almost thermoneutral for Ca, and endothermic for Mg) with a barrier varying in the 13–23 kcal/mol margins. The cyclic MCO_2 structure can further dissociate to MO+CO (via an OMOC intermediate for M=Be) and the overall $M+CO_2 \rightarrow MO+CO$ reactions were found to be endothermic by 26, 66, and 35 kcal/mol for M=Be, Mg, and Ca, respectively. For the case of Be, BeO, and CO can recombine giving the most stable OBeCO species, which lies ~11 kcal/mol lower in energy than Be $+CO_2$.

The $M+CO_2 \rightarrow MO+CO$ reaction scenario is quite different for early transition metals, in particular, for M=Sc. Sodupe *et al.*[24] showed that the Sc atom can insert into a CO bond to form OScCO practically without barrier. Our detailed DFT calculations[30] of the reaction PES revealed two possible mechanisms: insertion, $Sc+CO_2 \rightarrow \eta^2$-C,O (ScOC)O (−26.8 kcal/mol relative to the reactants) → TSi (−26.3) → end-OScCO (−38.1) → ScO+CO (−30.9), and addition, $Sc+CO_2 \rightarrow$ TS1 (3.2 kcal/mol) → η^1-O ScOCO (−3.8) → TS2 (−3.4) → η^2-O,O cyclic $ScCO_2$ (−27.3) → ScO+CO → side-OScCO (−33.8). While the insertion mechanism is clearly preferable kinetically, the addition may also contribute because the calculated barriers are rather low.

The insertion of Ti (s^2d^2, ^3F and s^1d^3, ^5F) into a CO bond of carbon dioxide was investigated by Papai *et al.*[26] who concluded that this process should occur without barrier yielding a OTiCO molecule. The high feasibility of the insertion was attributed to the Ti(3d)–$CO_2(3\pi^*)$ bonding interaction. Such interaction significantly decreases for late transition metals because of the strong contraction of the 3*d* orbitals and the increase of ionization potential as the atomic number increases.[26] Although Papai *et al.*[26] have calculated various $TiCO_2$ coordination complexes, no detailed study of the reaction mechanism of CO_2 with Ti in different electronic states has been reported so far. The goal of the present paper is to investigate the $Ti+CO_2$ reaction pathways, intermediates, and transition states and to compare reactivity of Ti atoms in the ground and excited electronic states.

II. COMPUTATIONAL DETAILS

We considered totally four electronic states for the $TiCO_2$ molecule, triplet (in most cases $^3A''$) correlated to the ground $Ti(3d^24s^2,{}^3F)+CO_2(^1\Sigma_g{}^+)$ states of the reactants, quintet ($^5A'$) correlated to $Ti(3d^34s^1,{}^5F)+CO_2(^1\Sigma_g{}^+)$, as well as closed shell ($^1A'$) and open shell ($^1A''$) singlets both correlated to $Ti(3d^24s^2,{}^1D)+CO_2(^1\Sigma_g{}^+)$. On these surfaces, full geometry optimizations were run to locate various stationary structures including local minima and first order saddle points at the B3LYP/6-31G* level.[31] Harmonic vibrational frequencies were obtained at the B3LYP/6-31G* level in order to characterize the stationary points as minima or transition states, to obtain zero-point vibration energy corrections (ZPE) and to generate force constant data needed in the intrinsic reaction coordinate (IRC) calculation. The IRC method[32] was used to track minimum energy paths from transition structures to the corresponding minimuma. A step size of 0.1 amu$^{1/2}$ bohr or larger was used in the IRC procedures. Details of the IRC calculations are given in the supplement to this paper.[33]

The relative energies were then refined by single point energy calculations with B3LYP/6-31G* optimized geometries using the B3LYP/6-311+G(3*df*) method with the larger and more flexible basis sets. In order to assess the expected accuracy of these procedures, we recalculated the energies of various electronic states of the Ti atom and TiO using the coupled cluster[34] CCSD(T)/6-311G* and CCSD(T)/6-311+G(3*df*) methods and multireference CASSCF[35] and MRCI[36] approaches with different active spaces and 6-311G* and 6-311+G(3*df*) basis sets. The calculations described here were performed employing the GAUSSIAN 98[37] and MOLPRO 2000[38] programs.

III. RESULTS AND DISCUSSION

The ground state total energies and relative energies of excited states for Ti and TiO calculated at various levels of theory are shown in Table I, the total and ZPE corrected relative energies of various compounds in the $Ti+CO_2$ reaction at the B3LYP/6-31G(*d*) and B3LYP/6-311+G(3*df*) levels of theory are listed in Table II. Table III presents vibrational frequencies obtained at the B3LYP/6-31G* level as well as their IR intensities and assignments of corresponding normal modes. The potential energy diagrams along the reaction pathways computed at the B3LYP/6-311+G(3*df*)//B3LYP/6-31G*+ZPE(B3LYP/6-31G*) level and the optimized geometric structures of various intermediates, transition states, and reaction products in triplet, singlet, and quintet electronic states are shown in Figs. 1–3, respectively.

A. Energy splitting between electronic states of Ti and TiO and the reaction energetics: Assessment of various levels of theory

According to experimental atomic spectra,[39] the lowest singlet and quintet states of the Ti atom are $3d^24s^2(^1D)$ and $3d^34s^1(^5F)$, which lie above the ground state triplet $3d^24s^2(^3F)$ state by 20.7 and 18.7 kcal/mol, respectively, if we consider the lowest spin–orbit component for each state. These values are difficult to reproduce both by DFT and single-reference CCSD(T) methods. The B3LYP and CCSD(T) calculations underestimate the ^1D energy by ~10 and 15–17 kcal/mol, while the basis set dependence is rather weak. Such underestimation apparently results from the spin contamination of the open shell singlet wave function by the lower energy triplet wave function; the $\langle \mathbf{S}^2 \rangle$ values are about 1.0 for UB3LYP and 1.5–1.6 for the UHF case. On the contrary, the CASSCF approach will full valence active space (4,9) overestimates the $^1D-{}^3F$ splitting by 7–9 kcal/mol but MRCI without and with Davidson corrections for quadruple excitations (MRCI+Q) performs much better. The difference between the best MRCI+Q(4,9)/6-311+G(3*df*) value and experiment is only 1.6 kcal/mol. Most of theoretical levels tend to overestimate the $^5F-{}^3F$ energy gap for the Ti atom. The best results are obtained by the CCSD(*T*)/6-311+G(3*df*) (22.0 kcal/mol), MRCI

TABLE I. Energy differences between ground and excited electronic states of Ti atom and TiO and heats of the $Ti+CO_2 \rightarrow TiO+CO$ reaction calculated at various levels of theory.

	$Ti(3d^24s^2,{}^3F)$[a]	$Ti(3d^24s^2,{}^1D)$[b]	$Ti(3d^34s^1,{}^5F)$[b]
B3LYP/6-31G*	−849.299 33	11.8	30.3
B3LYP/6-311G*	−849.344 09	11.7	25.7
B3LYP/6-311+G(3*df*)	−849.353 01	10.9	5.3
CCSD(T)/6-311G*	−848.388 97	4.2	24.7
CCSD(T)/6-311+G(3*df*)	−848.429 80	6.0	22.0
CASSCF(4,9)/6-311G*	−848.368 58	27.6	36.8
MRCI(4,9)/6-311G*	−848.382 59	23.1	24.6
MRCI+Q(4,9)/6-311G*	−848.382 71	23.1	20.1
CASSCF(4,9)/6-311+G(3*df*)	−848.400 27	29.4	38.4
MRCI(4,9)/6-311+G(3*df*)	−848.423 68	22.6	23.2
MRCI+Q(4,9)/6-311+G(3*df*)	−848.424 07	22.3	17.8
Experiment[c]		20.7	18.7
	$TiO({}^3\Delta)$[a]	$TiO({}^1\Delta)$[d]	$TiO({}^1\Sigma^+)$[d]
B3LYP/6-31G*	−924.614 48	4.9	21.3
B3LYP/6-311G*	−924.664 94	5.6	19.2
B3LYP/6-311+G(3*df*)	−924.700 61	5.7	25.3
CCSD(T)/6-311G*	−923.546 81	3.0	21.9
CCSD(T)/6-311+G(3*df*)	−923.639 90	3.0	18.5
CASSCF(10,10)/6-311G*	−923.384 77	11.0	24.7
MRCI(10,10)/6-311G*	−923.539 43	11.2	23.0
MRCI+Q(10,10)/6-311G*	−923.546 32	11.1	22.4
CASSCF(10,10)/6-311+G(3*df*)	−923.448 06	9.7	33.5
MRCI(10,10)/6-311+G(3*df*)	−923.627 30	9.5	22.4
MRCI+Q(10,10)/6-311+G(3*df*)	−923.637 19	9.1	18.4
CASSCF(10,16)/6-311G*	−923.430 42	11.2	19.2
CASSCF(10,16)/6-311+G(3*df*)	−923.493 24	10.1	17.8
Experiment[e]		9.8	16.2
ΔH_r $Ti+CO_2 \rightarrow TiO+CO$	$Ti({}^3F) \rightarrow TiO({}^3\Delta)$	$Ti({}^1D) \rightarrow TiO({}^1\Delta)$	$Ti({}^1D) \rightarrow TiO({}^1\Sigma^+)$
B3LYP/6-31G*	−30.0	−37.0	−20.6
B3LYP/6-311G*	−18.2	−24.3	−10.2
B3LYP/6-311+G(3*df*)	−30.1	−35.5	−15.9
CCSD(T)/6-311G*	−25.6	−26.8	−7.9
CCSD(T)/6-311+G(3*df*)	−25.1	−28.1	−12.6
Experiment[f]	−32.3	−43.2	−36.8

[a]Total energies in hartree.
[b]Relative energies in kcal/mol with respect to $Ti(3d^24s^2,{}^3F)$.
[c]From Ref. 38.
[d]Relative energies in kcal/mol with respect to $TiO({}^3\Delta)$.
[e]From Refs. 39 and 40.
[f]Based on experimental heats of formation for the ground state species (Ref. 27) and excitation energies for Ti and TiO.

+Q(4,9)6-311G* (20.1) and MRCI+Q(4,9)/6-311 +G(3*df*) (17.8) methods. Noteworthy, the correct energetic order of the ^1D and ^5F electronic states is reproduced only by MRCI calculations with Davidson corrections and by B3LYP/6-311+G(3*df*) but the latter significantly underestimates the energies of both states.

In experiment,[40,41] the three lowest electronic states of TiO are $^3\Delta$, $^1\Delta$, and $^1\Sigma^+$ with the last two lying by 9.8 and 16.2 kcal/mol, respectively, above the ground state. As seen in Figs. 1 and 2, the B3LYP/6-31G* calculations reproduced the experimental Ti–O bond lengths[27] with a good accuracy, uniformly underestimating them by ~0.02 Å. Correspondingly, the vibrational frequency in TiO is overestimated by 90–110 cm^{-1} (Table III). But the energy splittings are more difficult to calculate accurately. For the open shell singlet $^1\Delta$ state, B3LYP and CCSD(T) calculations underestimate the experimental value by 4–5 and ~7 kcal/mol, respectively, again due to the spin contamination. Both CASSCF and MRCI methods with the (10,10) active space (full valence active space excluding *p* orbitals of the Ti atom) gave the result within 1.3 kcal/mol from experiment and those with the large 6-311+G(3*df*) basis set provided even better accuracy. The $^1\Sigma^+ - {}^3\Delta$ energy gap is generally overestimated from 9.1 kcal/mol at B3LYP/6-311+G(3*df*) to 2.3 and 2.2 kcal/mol at CCSD(T)/6-311+G(3*df*) and MRCI +Q(10,10)/6-311+G(3*df*), respectively. The value closest to experiment (17.8 kcal/mol) is achieved by the CASSCF calculations with a very large (10,16) active space and the 6-311+G(3*df*) basis set. Interestingly, earlier Langhoff[42] obtained the relative energy of $^1\Sigma^+$ as 23.7 kcal/mol using similar internally contracted MRCI(8, 11) calculations with

TABLE II. Total energies (hartree), ZPE and relative energies (kcal/mol) of various species in the $Ti+CO_2$ reaction calculated at the B3LYP/6-31G* and B3LYP/6-311+G(3*df*)//B3LYP/6-31G* levels of theory.

	B3LYP/6-31G*			B3LYP/6-311+G(3*df*)	
Species	Total energy	ZPE	Relative energy	Total energy	Relative energy
CO_2	−188.580 94	7.28		−188.659 85	
t-Ti($3d^24s^2,{}^3F$)	−849.299 32			−849.353 01	
CO_2+*t*-Ti(^3F)	−1037.880 26	7.28	0	−1038.012 86	0
t-TS1($^3A''$)	−1037.870 71	5.55	4.27	−1038.002 56	4.74
t-cyc-$TiCO_2$($^3A''$)	−1037.911 68	5.71	−21.28	−1038.038 90	−17.91
t-TS2($^3A''$)	−1037.906 58	5.36	−18.43	−1038.032 65	−14.33
end-*t*-OTiOC($^3A''$)	−1037.929 40	5.28	−32.83	−1038.058 17	−30.43
side-*t*-OTiOC($^3A''$)	−1037.935 46	5.42	−36.50	−1038.060 07	−31.48
t-(TiOC)O($^3A''$)	−1037.917 22	6.59	−23.88	−1038.047 37	−22.34
t-TS3($^3A''$)	−1037.916 44	5.91	−24.07	−1038.045 94	−22.13
t-OTiCO($^3A''$)	−1037.952 54	5.90	−46.73	−1038.080 66	−43.92
t-TiO($^3\Delta$)	−924.614 50	1.57		−924.700 36	
CO	−113.309 45	3.16		−113.356 36	
t-TiO($^3\Delta$)+CO	−1037.923 95	4.72	−29.97	−1038.056 72	−30.08
q-Ti($3d^34s^1,{}^5F$)	−849.251 10			−849.344 50	
CO_2+*q*-Ti(^5F)	−1037.832 04	7.28	30.26	−1038.004 35	5.34
q-TS1($^5A'$)	−1037.847 68	6.03	19.20	−1037.995 69	9.53
q-cyc-$TiCO_2$($^5A'$)	−1037.881 22	6.56	−1.31	−1038.013 00	−0.80
q-TS2($^5A'$)	−1037.804 46	4.30	44.59	−1037.939 26	43.21
end-*q*-OTiOC($^5A'$)	−1037.815 18	4.51	38.07	−1037.949 95	36.71
q-(TiOC)O($^5A'$)	−1037.883 37	6.81	−2.42	−1038.019 11	−4.39
q-OTiCO($^5A'$)	−1037.848 67	5.38	17.92	−1037.982 03	17.45
q-TiOCO($^5A'$)	−1037.872 06	6.15	4.02	−1038.009 86	0.76
q-TiO($^5\Delta$)	−924.490 25	0.89		−924.578 34	
q-TiO(^{5})+CO	−1037.799 70	4.04	47.32	−1037.934 70	45.81
s-Ti($3d^24s^2,{}^1D$)	−849.280 48			−849.335 60	
s-Ti(^1D)+CO_2	−1037.861 42	7.28	11.82	−1037.995 45	10.92
s-TS1($^1A'$)	−1037.802 58	5.75	47.22	−1037.937 47	45.78
s-cyc-$TiCO_2$($^1A'$)	−1037.896 17	5.76	−11.50	−1038.011 65	−0.75
s-TS2($^1A'$)	−1037.884 37	5.44	−4.42	−1038.006 45	2.18
side-*s*-OTiOC(^1A)	−1037.936 71	5.76	−36.94	−1038.060 32	−31.30
s-(TiOC)O($^1A'$)	−1037.889 98	6.62	−6.75	−1038.017 04	−3.28
s-TS3($^1A'$)	−1037.889 42	6.00	−7.02	−1038.015 68	−3.05
s-OTiCO($^1A'$)	−1037.932 44	6.14	−33.88	−1038.067 77	−35.60
s-TS1($^1A''$)	−1037.850 45	5.45	16.88	−1037.981 79	17.67
s-cyc-$TiCO_2$($^1A''$)	−1037.896 53	5.61	−11.88	−1038.023 08	−8.08
s-TS2($^1A''$)	−1037.895 35	5.35	−11.40	−1038.020 90	−6.97
end-*s*-OTiOC($^1A''$)	−1037.922 84	5.36	−28.64	−1038.050 74	−25.69
s-TS3($^1A''$)	−1037.860 86	6.67	11.57	−1037.991 67	12.69
s-OTiCO($^1A''$)	−1037.947 57	6.00	−43.51	−1038.075 47	−40.56
s-TiO($^1\Delta$)	−924.606 76	1.58		−924.691 52	
s-TiO($^1\Delta$)+CO	−1037.916 21	4.74	−25.10	−1038.047 88	−24.52
s-TiO($^1\Sigma^+$)	−924.580 65	1.61		−924.660 48	
s-TiO($^1\Sigma^+$)+CO	−1037.890 10	4.77	−8.68	−1038.016 84	−5.01

an augmented Wachters basis set for Ti and aug-cc-pVTZ for O.

Let us now turn to the heat of the $Ti+CO_2 \rightarrow TiO+CO$ reaction. As seen in Table I, for the ground state triplet reaction the best results (within ~2 kcal/mol from experiment) are obtained at the B3LYP/6-31G* and B3LYP/6-311+G(3*df*) levels, while the CCSD(T) calculations underestimate the experimental exothermicity by ~7 kcal/mol. Naturally, due to the errors in excitation energies the performance of both B3LYP and CCSD(T) for excited singlet states is worse. For the open shell singlet reaction the B3LYP/6-31G* and B3LYP/6-311+G(3*df*) methods give the exothermicity 7–8 kcal/mol lower than in experiment and the error in CCSD(T) calculations increases to 15–16 kcal/mol. Finally, for the reaction involving the closed shell singlet state, the deviation of the B3LYP/6-311+G(3*df*) result from experiment exceeds 20 kcal/mol because the $^1D-{}^3F$ energy gap is underestimated by ~10 kcal/mol but $^3\Delta-{}^1\Sigma^+$ is overestimated by approximately the same amount.

Evidently, multireference MRCI calculations with large active spaces and basis sets is the most reliable way to provide chemical accuracy for the molecules containing excited state transition metal atoms. Unfortunately, such calculations are extremely demanding computationally and are not feasible at present. Among the alternative methods, the B3LYP/6-311+G(3*df*) approach is clearly preferable with respect to the much more costly CCSD(T) with the 6-311+G(3*df*) and 6-311G* basis sets because the former gives

TABLE III. Vibrational frequencies (cm^{-1}) of various compounds in the $Ti+CO_2 \rightarrow TiO+CO$ reaction calculated at the B3LYP/6-31G* level.[a]

Species	Frequencies
t-TS1($^3A''$)	510i, 80, 222, 364, 1107, 2110
t-cyc-$TiCO_2$($^3A''$)	349 (a'', 8.4, CO_2 off-plane wag), 371 (a', 13.7, TiO/CO str)
	439 (a', 15.8, TiO str), 724 (a', 22.7, CO_2 bend)
	1053 (a', 325.0, CO asym str), 1058 (a', 80.6, CO sym str)
t-TS2($^2A''$)	368i, 304, 411, 688, 856, 1491
end-t-OTiOC($^3A''$)	82 (a', 9.1, OTiO/TiOC bend), 156 (a'', 1.5, TiOC off-plane bend)
	166 (a', 15.1, OTi-OC str), 188 (a', 6.1, OTi-OC str/OTiO bend)
	1078 (a', 226.1, OTi str), 2025 (a', 123.7, CO str)
side-t-OTiOC(^3A)	139 (11.0, OTiO/TiOC bend), 176 (2.7, OTiOC torsion)
	300 (35.5, OTi-OC str), 360 (23.3, TiOC bend)
	1074 (313.8, TiO str), 1742 (24.0, CO str)
t-(TiOC)O($^3A''$)	339 (a', 9.9, OCO/TiCO bend), 383 (a', 19.6, Ti-OC str)
	385 (a'', 0.8, CO off-plane wag), 714 (a', 39.2, OCO bend)
	927 (a', 196.5, CO/TiC str), 1860 (a', 568.3, CO str)
t-TS3($^3A''$)	397i, 352, 357, 611, 908, 1904
t-OTiCO($^3A''$)	111 (a', 6.7, OTiC bend), 189 (a'', 11.5, TiCO off-plane bend)
	334 (a', 4.3, TiCO bend), 367 (a', 75.0 TiC str)
	1068 (a', 214.1, OTi str), 2058 (a', 2305.6, CO str)
t-TiO($^3\Delta$)	1093 [1009][b]
q-TS1($^5A'$)	873i, 64, 262, 480, 1144, 2269
q-cyc-$TiCO_2$($^5A'$)	171 (a', 3.0, TiO/CO str), 314 (a'', 2.8, CO_2 off-plane wag)
	375 (a', 68.4, TiO str), 797 (a', 46.5, CO_2 bend)
	1359 (a', 26.4, CO sym str), 1575 (a', 276.8, CO asym str)
q-TS2($^5A'$)	264i, 51, 89, 133, 611, 2124
end-q-OTiOC($^5A'$)	78 (a', 3.8, OTiO/TiOC bend), 189 (a'', 0.8, TiOC off-plane bend)
	207 (a'', 0.8, CO off-plane wag), 335 (a', 64.2, OTi-OC str)
	654 (a', 127.0, TiO str), 1690 (a', 1054.7, CO str)
q-(TiOC)O($^5A'$)	170 (a', 0.4, OCO/TiCO bend), 383 (a', 17.1, Ti-OC str)
	391 (a'', 3.5, CO_2 off-plane wag), 699 (a', 121.2, OCO bend)
	1193 (a', 96.8, CO/TiC str), 1925 (a', 371.6, CO str)
q-OTiCO($^5A'$)	86 (a', 8.0, OTiC/TiCO bend), 295 (a'', 0.0, TiCO off-plane bend)
	319 (a', 1.5, TiCO bend), 418 (a', 23.8, TiC str)
	644 (a', 121.8, OTi str), 2000 (a', 1438.9, CO str)
q-TiOCO($^5A'$)	67 (a'', 1.9, TiOC off-plane bend), 70 (a'', 0.7, TiOCO torsion)
	399 (a', 14.8, TiO str/CO_2 bend), 714 (a', 41.2, CO_2 bend)
	1203 (a', 60.0, asym str), 1848 (a', 767.2, sym str)
q-TiO($^5\Delta$)	620
s-TS1($^1A'$)	329i, 194, 217, 339, 1161, 2109
s-cyc-$TiCO_2$($^1A'$)	281 (a'', 0.0, CO_2 off-plane wag), 348 (a', 2.3, TiO/CO str)
	531 (a', 60.3, TiO str), 827 (a', 57.3, CO_2 bend)
	982 (a', 169.1, CO asym str), 1062 (a', 1.4, CO sym str)
s-TS2($^1A'$)	341i, 243, 449, 734, 909, 1468
side-s-OTiOC(^1A)	219 (17.8, OTiO bend), 261 (8.6, OTiOC torsion)
	429 (44.9, OTi–OC str), 493 (6.9, TiOC str/bend)
	1077 (218.4, TiO str), 1550 (225.0, CO str)
s-(TiOC)O($^1A'$)	298 (a', 0.2, TiCO/OCO bend), 391 (a'', 0.5, CO off-plane wag)
	429 (a', 39.0, Ti–OC str), 686 (a', 28.7, OCO bend)
	932 (a', 152.2, CO/TiC str), 1898 (a', 547.4, CO str)
s-TS3($^1A'$)	345i, 348, 362, 600, 931, 1956
s-OTiCO($^1A'$)	135 (a', 19.2, OTiC/TiCO bend), 271 (a'', 83.7, TiCO off-plane bend)
	339 (a', 1.6, TiCO bend), 508 (a', 4.2, TiC str)
	1058 (a', 252.2, OTi str), 1981 (a', 581.9, CO str)
s-TiO($^1\Sigma^+$)	1125 [1014][b]
s-TS1($^1A''$)	553i, 88, 203, 349, 1082, 2090
s-cyc-$TiCO_2$($^1A''$)	245 (a', 18.3, TiO/CO str), 364 (a'', 5.9, CO_2 off-plane wag)
	495 (a', 55.4, TiO str), 756 (a', 2.5, CO_2 bend)
	1004 (a', 259.7, CO asym str), 1060 (a', 18.9, CO sym str)
s-TS2($^1A''$)	290i, 327, 447, 708, 861, 1397
end-s-OTiOC($^1A''$)	91 (a', 7.6, OTiO/TiOC bend), 178 (a', 13.1, TiOC bend)
	188 (a'', 2.2, TiOC off-plane bend), 203 (a'', 15.3, OTiOC torsion)
	1088 (a', 201.0, OTi str), 1999 (a', 204.9, CO str)

TABLE III. (*Continued*.)

Species	Frequencies
s-TS3($^1A''$)	163*i*, 123, 451, 454, 1280, 2357
s-OTiCO($^1A''$)	110 (a', 6.4, OTiC/TiCO bend), 246 (a'', 0.8, TiCO off-plane bend)
	334 (a', 5.2, TiCO bend), 377 (a', 62.9, TiC str)
	1077 (a', 201.8, OTi str), 2051 (a', 2322.8, CO str)
s-TiO($^1\Delta$)	1104 [1009][b]

[a]In parentheses: symmetry, IR intensity (kM/mol), and assignment of the normal mode.
[b]In brackets: experimental frequency from Ref. 27.

a qualitatively correct energetic order of electronic states of the Ti atom, provides a better accuracy than the latter for the energy splittings between the $^3\Delta$, $^1\Delta$, and $^1\Sigma^+$ states of TiO, and reproduces the experimental heat of the ground state triplet $Ti+CO_2 \rightarrow TiO+CO$ reaction within a ~2 kcal/mol margin. While using the B3LYP/6-311+G(3*df*) method for the singlet and quintet reactions, we have to keep in mind that for the species at the initial reaction steps the energy differences between triplet and singlet and triplet and quintet are underestimated, while that between quintet and singlet may be slightly overestimated. Another general trend is that our calculations are expected to give too low energies for the $^1A''$ species owing to the spin contamination.

B. Reaction mechanism in the ground triplet electronic state

As seen in Fig. 1, PES for the triplet state reaction pathway is the lowest in energy and thus the most important. Similarly to the $Sc(^2D)+CO_2$ reaction,[30] two mechanisms are possible for $Ti+CO_2$, which can be called as insertion and addition mechanisms. At the initial reaction step in the insertion mechanism, the triplet Ti atom attaches to the carbon dioxide with formation of a planar η^2-C,O *t*-(TiOC)O ($^3A''$) intermediate without exit barrier. *t*-(TiOC)O is stabilized by 22.4 kcal/mol relative to reactants $Ti(^3F)+CO_2$. From the *t*-(TiOC)O intermediate the reaction proceeds by insertion of the Ti atom into the CO bond to produce *t*-OTiCO ($^3A''$) via an early transition state *t*-TS3. The B3LYP/6-311+G(3*df*)//B3LYP/6-31G* calculated insertion barrier is only 0.2 kcal/mol and the exothermicity of the *t*-(TiOC)O→*t*-OTiCO reaction step is 21.6 kcal/mol. The transition state optimization was followed by frequency and IRC calculations at the B3LYP/6-31G* level of theory which confirmed that *t*-TS3 connects *t*-(TiOC)O and *t*-OTiCO. The latter can decompose to TiO+CO without exit barrier and with endothermicity of 13.8 kcal/mol. Interest-

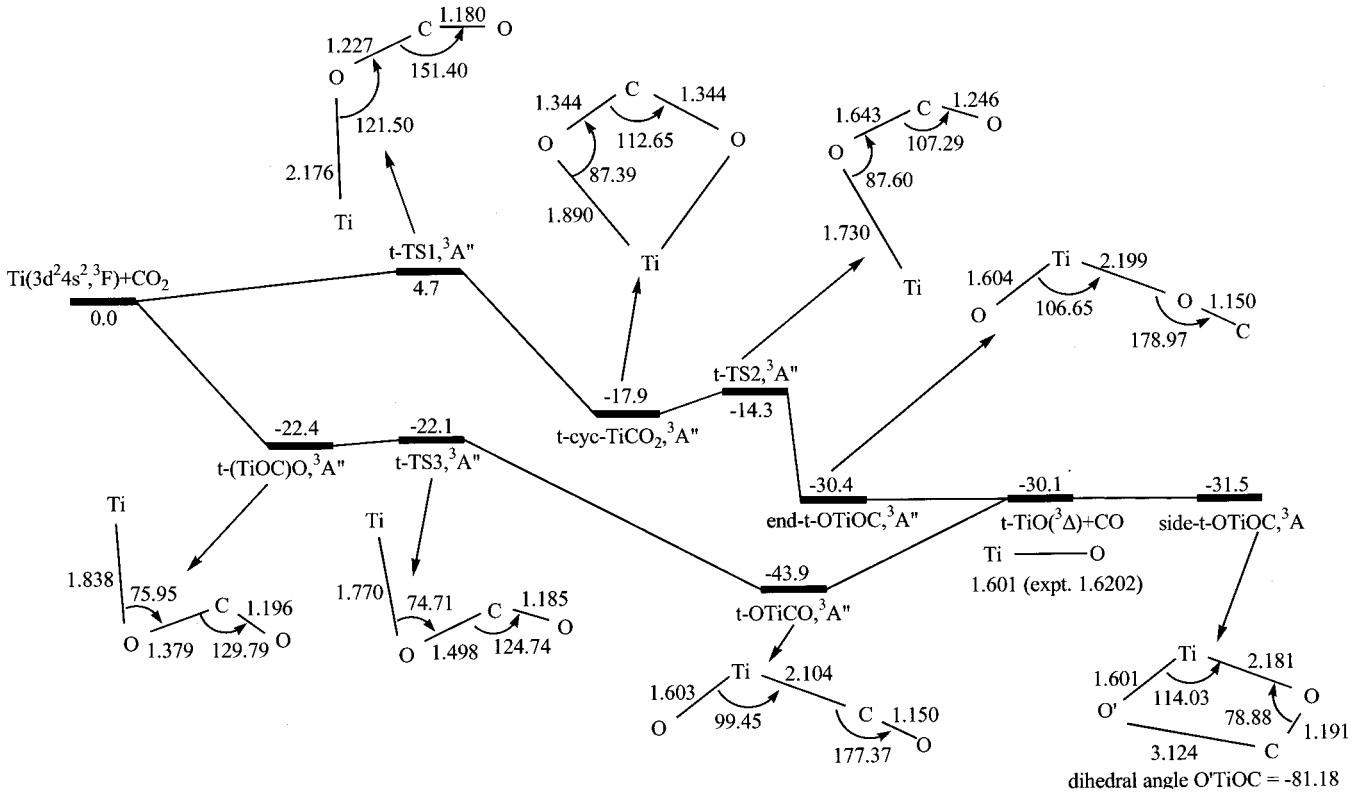

FIG. 1. Potential energy diagram for the $Ti+CO_2 \rightarrow TiO+CO$ reaction in triplet electronic state calculated at the B3LYP/6-311+G(3*df*)//B3LYP/6-31G*+ZPE(B3LYP/6-31G*) level and B3LYP/6-31G* optimized geometries of corresponding intermediates, transition states, and products. (Bond lengths are in Å and bond angles are in degrees.)

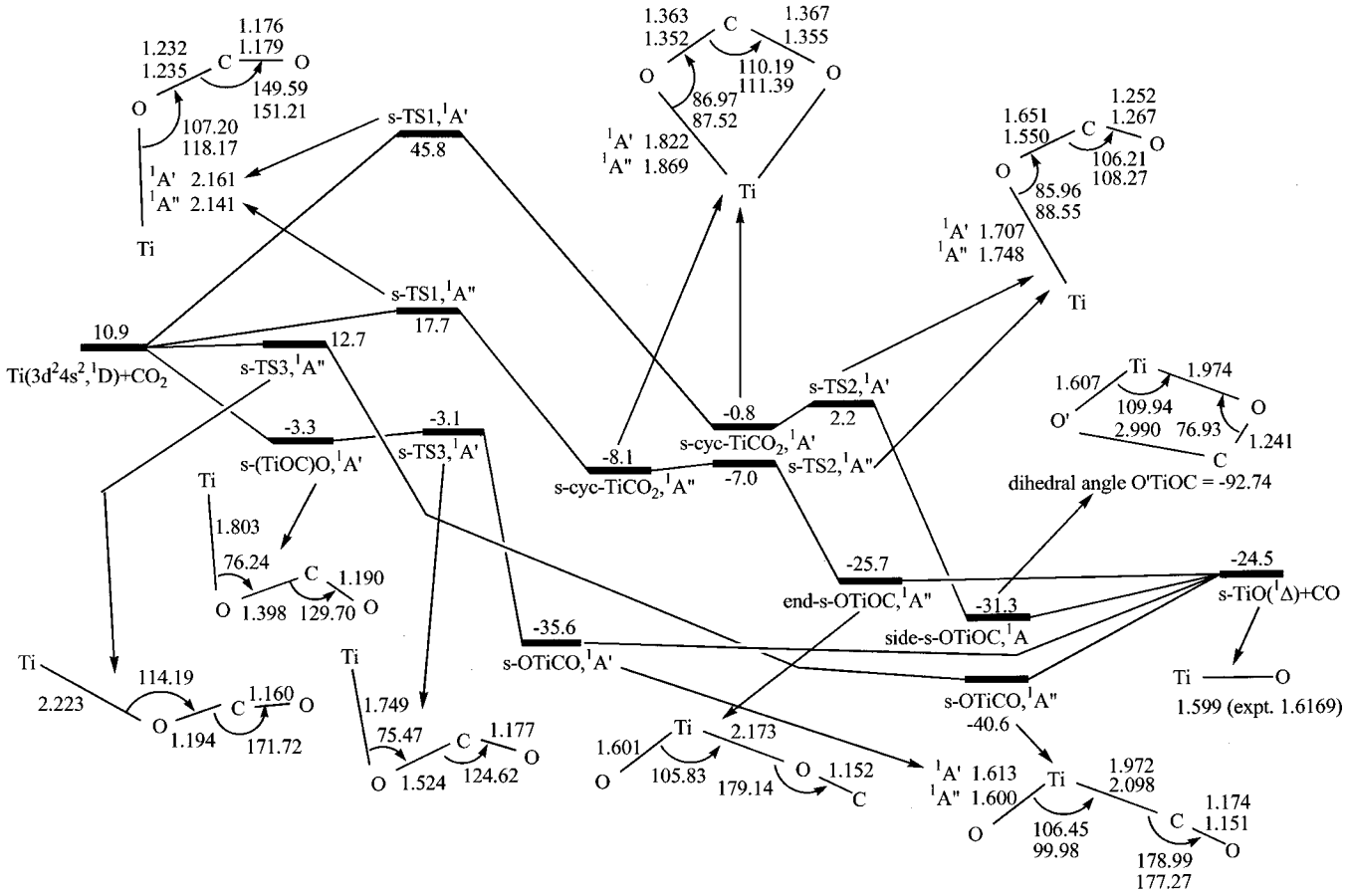

FIG. 2. Potential energy diagram for the $Ti+CO_2 \rightarrow TiO+CO$ reaction in singlet electronic state calculated at the B3LYP/6-311 $+G(3df)$//B3LYP/6-31G*+ZPE(B3LYP/6-31G*) level and B3LYP/6-31G* optimized geometries of corresponding intermediates, transition states, and products. (Bond lengths are in Å and bond angles are in degrees.)

ingly, the complex formation energy of η^2-C,O *t*-(TiOC)O from triplet Ti and CO_2, 22.3 kcal/mol, is somewhat lower than that for η^2-C,O *t*-(ScOC)O, 28.3 kcal/mol at the same level of theory.[30] On the other hand, *t*-OTiCO is predicted to be more stable than OScCO, since the former lies 43.9 and 13.8 kcal/mol lower in energy than $Ti(^3F)+CO_2$ and $TiO(^3\Delta)+CO$, respectively, as compared to 38.7 and 6.9 kcal/mol for the corresponding relative energies of OScCO.[30]

In the addition reaction mechanism, the triplet Ti atom attaches to CO_2 with formation of a planar cyclic nearly C_{2v}-symmetric η^2-O,O *t*-cyc-$TiCO_2$ intermediate ($^3A''$) through *t*-TS1 with exothermicity of 17.9 kcal/mol. The activation barrier for this step is quite low, 4.7 kcal/mol. IRC calculations confirmed that TS1 is connected to *t*-cyc-$TiCO_2$ in the forward direction. The IRC pathway in the reverse direction led to the reactants, $Ti(^3F)+CO_2$, and no η^1-O TiOCO complex was found. Papai *et al.*[26] reported such a complex in the triplet state but its energy was ~42 kcal/mol higher than the energy of the triplet η^2-O,O complex. Therefore, even if the η^1-O TiOCO complex may exist, it is not expected to play a significant role in the $Ti(^3F)+CO_2$ reaction. Our B3LYP/6-31G* calculations gave no local minima with a η^1-O TiOCO structure in the triplet electronic states. From the *t*-cyc-$TiCO_2$ intermediate the reaction proceeds to produce a *t*-OTiOC complex via transition state *t*-TS2. In this process, one TiO and one CO bonds break apart and TiO is coordinated towards the oxygen atom of carbon monoxide. The transition state *t*-TS2 exhibits a rather early character and the barrier for this reaction step is only 3.6 kcal/mol. We found two coordination modes of TiO with respect to OC in the *t*-OTiOC complex, a planar end-on structure $^3A''$ and a nonplanar side-on ^3A configuration. Both complexes are only slightly bound with respect to the products, $TiO(^3\Delta)+CO$, by 0.3 and 1.4 kcal/mol, respectively. The side-*t*-OTiOC structure is a little more stable but according to the IRC calculations *t*-TS2 connects *t*-cyc-$TiCO_2$ with the planar end-*t*-OTiOC complex, which, in turn, would easily dissociate to $TiO(^3\Delta)+CO$.

Comparison of the insertion and addition reaction mechanisms of the $Ti(^3F)+CO_2 \rightarrow TiO(^3\Delta)+CO$ shows that the former should be favored at low temperatures since it does not have any transition states lying higher in energy than the reactants. The addition mechanism can contribute into the reaction at ambient temperatures because the calculated barrier at TS1 is not very high, 4.7 kcal/mol. Apparently, only the *t*-OTiCO intermediate can be detectable in this reaction; the kinetic stability of the *t*-(TiOC)O and *t*-OTiOC species is expected to be very low. *t*-cyc-$TiCO_2$ is stabilized by a 3.6 kcal/mol barrier and might by found at very low temperatures but in this case the reaction is not likely to follow the addition mechanism via this intermediate. For the reverse $TiO(^3\Delta)+CO$ reaction the most likely

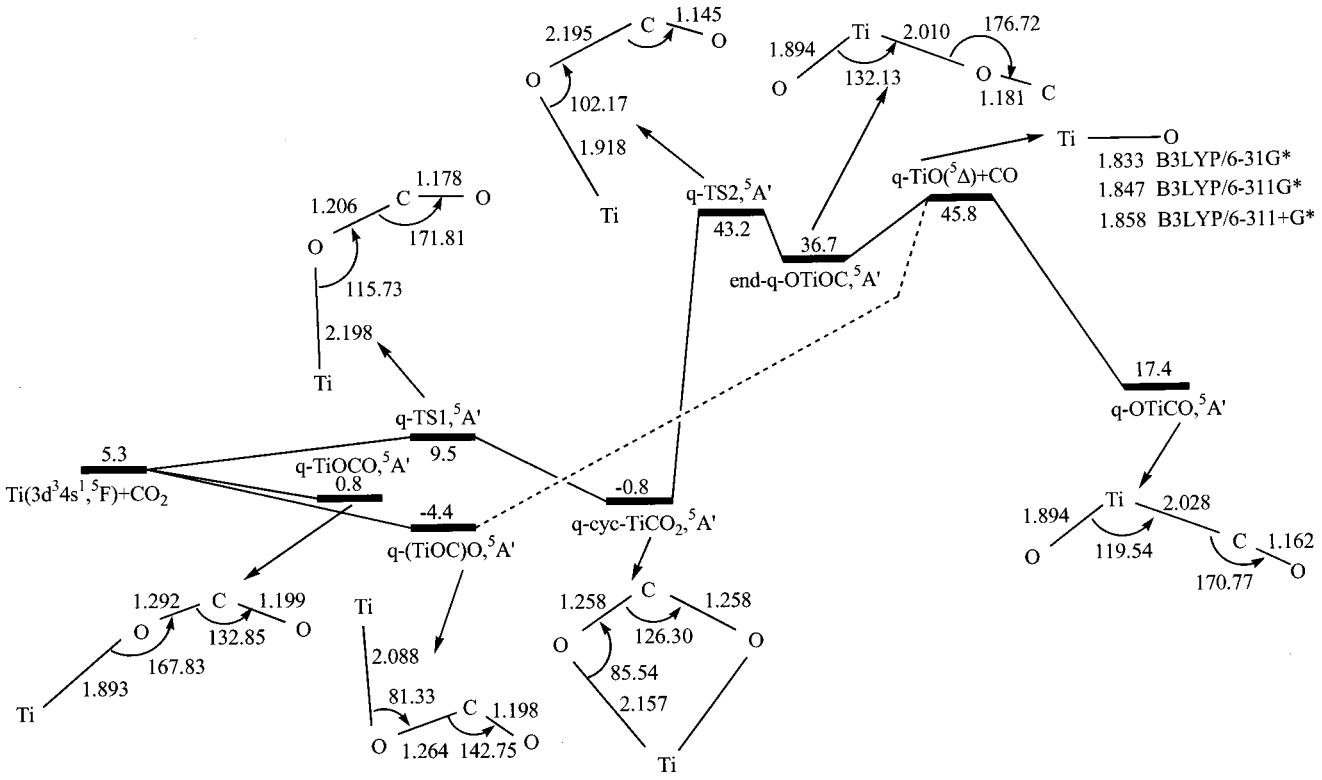

FIG. 3. Potential energy diagram for the $Ti+CO_2 \rightarrow TiO+CO$ reaction in quintet electronic state calculated at the B3LYP/6-311 $+G(3df)$//B3LYP/6-31G*+ZPE(B3LYP/6-31G*) level and B3LYP/6-31G* optimized geometries of corresponding intermediates, transition states, and products. (Bond lengths are in Å and bond angles are in degrees.)

product is *t*-OTiCO, which can be formed without barrier and with exothermicity of 13.8 kcal/mol. Since all other reaction steps are endothermic and have high barriers, they can take place only at high temperatures.

C. Reaction mechanisms in the excited quintet and singlet electronic states

Although the $Ti+CO_2$ reactions in excited electronic states depict many similarities with the ground state reaction, each electronic state shows some specific features. In the singlet state (Fig. 2), PES of infinitely separated reactants, $Ti(^1D)+CO_2$, has a fivefold degeneracy, while the $TiO(^1\Delta)+CO$ products at the infinite separation have a doubly degenerate electronic state. Hence, two surfaces can connect $Ti(^1D)+CO_2$ with $TiO(^1\Delta)+CO$. In the open shell singlet $^1A''$ state, the insertion mechanism PES shows no η^2-C,O (TiOC)O intermediate and the reaction proceeds directly from the $Ti(^1D)+CO_2$ reactants to the *s*-OTiCO ($^1A''$) molecule via transition state *s*-TS3 ($^1A''$) with a barrier of 1.8 kcal/mol. *s*-OTiCO ($^1A''$) resides 51.5 kcal/mol below the reactants and is calculated to be only 3.3 kcal/mol less stable than *t*-OTiCO ($^3A''$). The *s*-OTiCO ($^1A''$) intermediate is stabilized relative to $TiO(^1\Delta)+CO$ by 16.1 kcal/mol and, as in the triplet state, the Ti–C bond breaks without an exit barrier. In the addition mechanism, the calculated barrier to produce *s*-cyc-$TiCO_2$ ($^1A''$) via *s*-TS1 ($^1A''$) is 6.8 kcal/mol, ~2 kcal/mol higher than that for the triplet state. The rest of the addition pathway PES in the $^1A''$ state replicates the corresponding $^3A''$ surface with the energies of all intermediates and transition states up-shifted by 5–10 kcal/mol.

In the closed shell singlet electronic state ($^1A'$), the insertion pathway is similar to that in the triplet state. The *s*-(TiOC)O ($^1A'$) complex is formed initially without an entrance barrier and with the energy gain of 14.2 kcal/mol, ~8 kcal/mol smaller than the complex formation energy in the $^3A''$ state. The insertion barrier to yield *s*-OTiCO ($^1A'$) is only 0.2 kcal/mol. The *s*-OTiCO ($^1A'$) intermediate lies 46.5 kcal/mol below the reactants and is 8.3 and 5.0 kcal/mol less stable than *t*-OTiCO ($^3A''$) and *s*-OTiCO ($^1A''$), respectively. The stabilization energy of *s*-OTiCO ($^1A'$) relative to $TiO(^1\Delta)+CO$ is calculated as 11.1 kcal/mol, but this value may be slightly underestimated since the B3LYP/6-311 $+G(3df)$ method underestimates the $^1\Delta-^3\Delta$ splitting in TiO by ~4 kcal/mol. A peculiar feature of the addition mechanism for the $^1A'$ electronic state is the appearance of a high barrier, 34.9 kcal/mol, at *s*-TS1 ($^1A'$). Our B3LYP/6-311+G(3*df*) calculations may overestimate the barrier height since they give ~10 kcal/mol too low energy for the singlet $Ti(^1D)$ atom. The addition leads to the *s*-cyc-$TiCO_2$ ($^1A'$) complex, 11.7 kcal/mol below the reactants, which would quickly rearrange to *s*-OTiOC (^1A) clearing a barrier of 3.0 kcal/mol at *s*-TS2 ($^1A'$). In the closed shell singlet state *s*-OTiOC has a nonplanar geometry with a side-on configuration and can decompose to $TiO(^1\Delta)+CO$ losing 6.8 kcal/mol.

On the contrary to the exothermic triplet and singlet reactions, the $Ti(^5F)+CO_2 \rightarrow TiO(^5\Delta)+CO$ reaction in the quintet state is calculated to be 40.5 kcal/mol endothermic at the B3LYP/6-311+G(3*df*)//B3LYP/6-31G*+ZPE level. This fact significantly affects the reaction mechanism (see Fig. 3). Along the ''insertion'' pathway, the *q*-(TiOC)O complex can be formed without a barrier and with an energy gain of 9.7 kcal/mol. But the insertion itself requires high energy expenses. The *q*-OTiCO molecule is a local minimum but it lies 61.3 kcal/mol above the most stable triplet *t*-OTiCO ($^3A''$) configuration and 12.1 kcal/mol higher in energy than the reactants. We were not able to locate a *q*-TS3 transition state between *q*-(TiOC)O and *q*-OTiCO. Possibly, the *q*-(TiOC)O intermediate has to first decompose to $TiO(^5\Delta)+CO$, which can then recombine to *q*-OTiCO without a barrier and with exothermicity of 28.4 kcal/mol. Along the addition pathway, $Ti(^5F)+CO_2$ produce *q*-cyc-$TiCO_2$ with an energy gain of 6.1 kcal/mol via a barrier of 4.2 kcal/mol at *q*-TS1. Further transformation of the *q*-cyc-$TiCO_2$ intermediate is hindered by a high barrier (44 kcal/mol) at *q*-TS2. If this barrier can be cleared at high temperatures, a planar end-*q*-OTiOC intermediate will be formed, stabilized by 9.1 kcal/mol with respect to $TiO(^5\Delta)+CO$. The end-*q*-OTiOC complex can decompose to the quintet TiO and carbon monoxide without an exit barrier. Essentially, the *q*-(TiOC)O and *q*-cyc-$TiCO_2$ intermediates represent ''dead ends'' on the quintet PES. The former can be produced even at very low temperatures (no barrier), while the latter can be yielded at ambient temperatures when the ~4 kcal/mol barrier can be overcome. Additionally, the quintet Ti atom can coordinate toward CO_2 in the η^1-O manner to form without a barrier a *q*-TiOCO ($^5A'$) complex bound by 4.6 kcal/mol.

A comparison of PES for various electronic states shows that the Ti atom is expected to be most reactive with respect to carbon dioxide in the ground triplet electronic state. The most probable reaction mechanism in this case is the Ti insertion into a CO bond and the most likely primary reaction products would be *t*-OTiCO ($^3A''$) and $TiO(^3\Delta)+CO$. In the singlet state, the reaction most favorable pathway is the barrierless insertion along the $^1A'$ PES leading to *s*-OTiCO ($^1A'$) and eventually to $TiO(^1\Delta)+CO$. Insertion on the open shell singlet $^1A''$ PES requires to overcome a low barrier of 1.8 kcal/mol and yields *s*-OTiCO ($^1A''$) and $TiO(^1\Delta)+CO$. The addition barriers to form the *s*-cyc(TiOC)O complexes in the $^1A''$ and $^1A'$ singlet states are higher than the corresponding barrier on the $^3A''$ surface, especially, for $^1A'$. In the quintet state, the only facile products are relatively weakly bound *q*-(TiOC)O, *q*-cyc-$TiCO_2$, and *q*-TiOCO complexes and the reaction is not expected to proceed further to *q*-OTiCO or $TiO(^5\Delta)+CO$.

Based on a comparison of calculated and experimental vibrational frequencies and isotopic shifts for singlet and triplet OTiCO, Papai *et al.*[26] concluded that the singlet state insertion product was observed in the matrix isolation experiment. The experimental CO and TiO stretching frequencies are 1867 and 953 cm^{-1}, respectively,[22] and the BP86 frequencies obtained by Papai *et al.* are 1881 and 967 cm^{-1} for singlet and 1986 and 991 cm^{-1} for triplet.[26] If we scale our B3LYP/6-31G* frequencies (Table III) by a factor 0.9614 as suggested by Scott and Radom,[43] we obtain 1979 and 1027 cm^{-1} for the $^3A''$ state, 1972 and 1035 cm^{-1} for $^1A''$, and 1905 and 944 cm^{-1} for $^1A'$. The agreement with experiment for the $^1A'$ state is indeed slightly better but the difference may be within the error margins of the calculations. According to the calculated PES *t*-OTiCO is most likely to be produced although (allowing for singlet–triplet intersystem crossing) singlet OTiCO can be also formed. Further studies would be needed to clarify this matter. Interestingly, the *t*-(TiOC)O complex has the frequencies quite close to the experimental values (1860 and 927 cm^{-1}, unscaled) but this intermediate is not expected to be very stable kinetically.

IV. CONCLUDING REMARKS

Density functional B3LYP/6-311+G(3*df*)//B3LYP/6-31G* calculations of PES for the $Ti+CO_2 \rightarrow TiO+CO$ reaction show that in the ground electronic state the most favorable energetically reaction mechanism is insertion of the Ti atom into a CO bond [via a η^2-C,O coordinated (TiOC)O complex] to produce the triplet OTiCO molecule with exothermicity of 43.9 kcal/mol. The latter can further dissociate to $TiO(^3\Delta)+CO$. The total reaction exothermicity is calculated as 30.1 kcal/mol, in close agreement with the experimental value of 32.3 kcal/mol.[27] The addition mechanism leading to the same $TiO(^3\Delta)+CO$ products via a metastable η^2-O,O complex *t*-cyc-$TiCO_2$ is also feasible since the transition state corresponding to the highest barrier on the reaction pathway lies 4.7 kcal/mol above the reactants. At ambient temperatures the two reaction mechanisms can compete.

The reaction mechanisms in excited singlet and quintet electronic states have many similar features with the ground state reaction but also exhibit some differences. In the singlet state, the reaction can follow open shell $^1A''$ and close shell $^1A'$ pathways, of those the insertion via the *s*-(TiOC)O ($^1A'$) complex leading to *s*-OTiCO ($^1A'$) and then to $TiO(^1\Delta)+CO$ does not require activation and is therefore most favorable. The insertion mechanism on the $^1A''$ PES has a low barrier of 1.8 kcal/mol and leads to *s*-OTiCO ($^1A''$), which also decomposes to $TiO(^1\Delta)+CO$. The addition pathways via the η^2-O,O coordinated complex require clearing significant barriers, 7.8 and 34.9 kcal/mol for the $^1A''$ and $^1A'$ states, respectively. In the quintet state, the reaction can proceed (at least, at low and ambient temperatures) only by coordination of $Ti(^5F)$ toward carbon dioxide with formation of η^2-C,O *q*-(TiOC)O, η^2-O,O *q*-cyc-$TiCO_2$, and η^1-O *q*-TiOCO bound by 9.7, 6.1, and 4.6, respectively, relative to the reactants. The η^2-C,O and η^1-O coordinations occur without barriers, while the η^2-O,O coordination shows an entrance barrier of 4.2 kcal/mol. Production of the quintet *q*-OTiCO molecule and $TiO(^5\Delta)+CO$ is significantly endothermic and therefore may occur only at high temperatures.

A comparison of the $M+CO_2 \rightarrow MO+CO$ PES and reaction mechanisms for various metal atoms M (alkaline–earth, early and late transition metals)[28–30] indicates that although all of them can enhance CO_2 reforming into carbon monoxide, the early transition metals (like Sc and Ti) are the best for this purpose. The $Ti+CO_2 \rightarrow TiO+CO$ and $Sc+CO_2 \rightarrow ScO+CO$[30] reactions are ~30–35 kcal/mol exo-

thermic and do not have activation barriers. Therefore, the carbon dioxide conversion into CO in the presence of Ti and Sc can occur spontaneously. The alkaline earth (Be, Mg, Ca)[29] and late transition metals (Ni)[28] although reduce the activation energy needed for the $CO_2 \rightarrow CO$ transformation[44] remain endothermic and the highest barriers on the reaction pathway are in the 25–70 kcal/mol range.

We have also assessed the accuracy of various *ab initio* and DFT methods, including B3LYP, CCSD(T), CASSCF, and MRCI, for calculations of energy splittings between various electronic states of Ti and TiO. As could be expected, the MRCI approach gives the most accurate results, within 1–2 kcal/mol from experiment. Neither B3LYP nor CCSD(T) are able to provide such an accuracy. On the other hand, the B3LYP/6-311+G(3*df*)//B3LYP/6-31G* method is expected to be preferable as compared to the more costly CCSD(T) for molecules containing Ti atoms because it gives more accurate results for the energy differences between various electronic states of Ti and TiO and for the heat of the $Ti + CO_2 \rightarrow TiO + CO$ reaction.

ACKNOWLEDGMENTS

Funding from Tamkang University was used to buy the computer equipment used in part of this investigation. A partial support from Academia Sinica and from the National Science Council of Taiwan, ROC, is also appreciated.

[1] K. Tanabe, in *Catalysis, Science and Technology*, edited by J. R. Anderson and M. Boudart (Springer-Verlag, New York, 1981).
[2] K. J. Klabunde, R. A. Kaba and R. M. Morris, in *Inorganic Compounds with Unusual Properties-II*, edited by R. B. King (American Chemical Society, Washington, DC, 1979), Adv. Chem. Ser. No. 173.
[3] *Studies in Surface Science and Catalysis 21. Adsorption and Catalysis on Oxide Surfaces*, edited by M. Che and G. C. Bond (Elsevier, Amsterdam, 1985).
[4] J. Mascetti and M. Tranquille, J. Phys. Chem. **92**, 2177 (1988).
[5] J. E. Benett, B. Mile, and A. Thomas, Trans. Faraday Soc. **61**, 2357 (1965).
[6] M. E. Jacox, and D. E. Mulligan, Chem. Phys. Lett. **28**, 163 (1974).
[7] J. P. Borel, F. Faes, and A. Pittet, J. Chem. Phys. **74**, 2120 (1981).
[8] R. H. Hauge, J. L. Margrave, J. W. Kauffmann, N. A. Rao, M. M. Konarski, J. P. Bell, and W. E. Billups, J. Chem. Soc. Chem. Commun. **1983**, 1528.
[9] Z. H. Kafafi, R. H. Hauge, W. E. Billups, and J. L. Margrave, J. Am. Chem. Soc. **105**, 3886 (1983).
[10] Z. H. Kafafi, R. H. Hauge, W. E. Billups, and J. L. Margrave, Inorg. Chem. **23**, 177 (1984).
[11] R. Teghil, B. Janis, and L. Bencivenni, Inorg. Chim. Acta **88**, 115 (1984).
[12] J. Bentley and I. J. Carmichael, J. Phys. Chem. **89**, 4040 (1985).
[13] G. A. Ozin, H. Huber, and D. McIntosh, Inorg. Chem. **17**, 1472 (1978).
[14] H. Huber, D. McIntosh, and G. A. Ozin, Inorg. Chem. **16**, 975 (1977).
[15] Y. Yoshioka and K. D. Jordan, Chem. Phys. Lett. **84**, 370 (1981); K. D. Jordan, J. Phys. Chem. **88**, 2459 (1984); F. Ramondo, N. Sanna, L. Bencivenni, and F. Grandinetti, Chem. Phys. Lett. **180**, 369 (1991).
[16] R. Caballol, E. S. Marcos, and J. C. Barthelat, J. Phys. Chem. **91**, 1328 (1987).
[17] G.-H. Jeung, Mol. Phys. **65**, 669 (1988); *ibid.* **67**, 747 (1989); Chem. Phys. Lett. **232**, 319 (1995).
[18] A. M. Le Quere, C. Xu, and L. Manceron, J. Phys. Chem. **95**, 3031 (1991).
[19] L. Andrews and T. J. Tague, Jr., J. Am. Chem. Soc. **116**, 6856 (1994).
[20] T. R. Burkholder, L. Andrews, and R. J. Bartlett, J. Phys. Chem. **97**, 3500 (1993).
[21] M. Zhou and L. Andrews, J. Am. Chem. Soc. **120**, 13230 (1998).
[22] G. V. Chertihin and L. Andrews, J. Am. Chem. Soc. **117**, 1595 (1995).
[23] P. F. Souter and L. Andrews, J. Am. Chem. Soc. **119**, 7350 (1997).
[24] M. Sodupe, V. Branchadell, and A. Oliva, J. Phys. Chem. **99**, 8567 (1995); L. Rodriguez-Santiago, M. Sodupe, and V. Branchadell, J. Chem. Phys. **105**, 9966 (1996); M. Sodupe, V. Branchadell, and A. Oliva, J. Mol. Struct.: THEOCHEM **371**, 79 (1996).
[25] F. Galan, M. Fouassier, M. Tranquille, J. Mascetti, and L. Papai, J. Phys. Chem. A **101**, 2626 (1997).
[26] I. Papai, J. Mascetti, and R. Fournie, J. Phys. Chem. A **101**, 4465 (1997).
[27] NIST Chemistry Webbook, NIST Standard Reference Data Base Number 69, February 2000 Release. http://webbook.nist.gov/chemistry/
[28] A. M. Mebel and D.-Y. Hwang, J. Phys. Chem. A **104**, 11622 (2000).
[29] D.-Y. Hwang and A. M. Mebel, J. Phys. Chem. A **104**, 7646 (2000); Chem. Phys. Lett. **325**, 639 (2000); *ibid.* **331**, 526 (2000).
[30] D.-Y. Hwang and A. M. Mebel, Chem. Phys. Lett. (in press).
[31] A. D. Becke, J. Chem. Phys. **98**, 5648 (1993); C. Lee, W. Yang, and R. G. Parr, Phys. Rev. B **37**, 785 (1988).
[32] C. Gonzales and H. B. Schlegel, J. Chem. Phys. **90**, 2154 (1989).
[33] See EPAPS Document No. E-JCPSA6-116-303213 for details of the IRC calculations. This document may be retrieved via the EPAPS homepage (http://www.aip.org/pubservs/epaps.html) or from ftp.aip.org in the directory /epaps/. See the EPAPS homepage for more information.
[34] G. D. Purvis and R. J. Bartlett, J. Chem. Phys. **76**, 1910 (1982).
[35] H.-J. Werner and P. J. Knowles, J. Chem. Phys. **82**, 5053 (1985). P. J. Knowles and H.-J. Werner, Chem. Phys. Lett. **115**, 259 (1985).
[36] H.-J. Werner and P. J. Knowles, J. Chem. Phys. **89**, 5803 (1988); P. J. Knowles and H.-J. Werner, Chem. Phys. Lett. **145**, 514 (1988).
[37] M. J. Frisch, G. W. Trucks, H. B. Schlegel *et al.*, GAUSSIAN 98, Revision A.7, Gaussian, Inc., Pittsburgh, PA, 1998.
[38] MOLPRO is a package of *ab initio* programs written by H.-J. Werner and P. Knowles with contributions from J. Almlöf, R. D. Amos, M. J. O. Deegan, S. T. Elbert, C. Hampel, W. Meyer, K. Peterson, R. Pitzer, A. J. Stone, P. R. Taylor, and R. Lindh.
[39] S. E. Moore, *Atomic Energy Levels* (NSRDS, Washington, D.C., 1971).
[40] H. Wu and L.-S. Wang, J. Chem. Phys. **107**, 8221 (1997).
[41] D. W. Schwenke, Faraday Discuss. **109**, 321 (1998).
[42] S. P. Langhoff, Astrophys. J. **481**, 1007 (1997).
[43] A. P. Scott and L. Radom, J. Phys. Chem. **100**, 16502 (1996).
[44] D.-Y. Hwang and A. M. Mebel, Chem. Phys. **256**, 169 (2000).